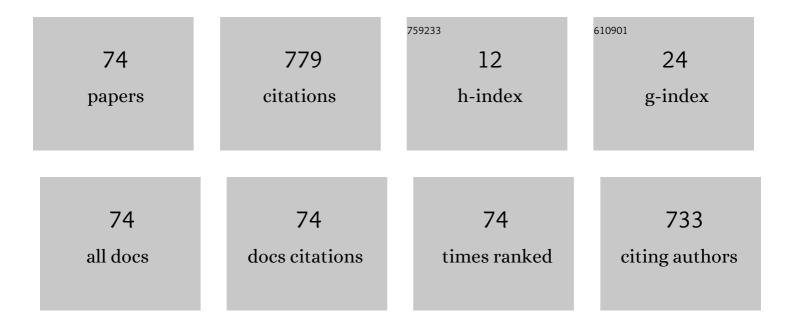
Tetsuya Takakuwa

List of Publications by Year in descending order

Source: https://exaly.com/author-pdf/7018315/publications.pdf Version: 2024-02-01



#	Article	IF	CITATIONS
1	Three-Dimensional Analysis of Human Laryngeal and Tracheobronchial Cartilages during the Late Embryonic and Early Fetal Period. Cells Tissues Organs, 2022, 211, 1-15.	2.3	3
2	Skeletal System Analysis during the Human Embryonic Period Based on MCA. , 2022, , 113-119.		0
3	MCA-Based Embryology and Embryo Imaging. , 2022, , 121-130.		0
4	Three-Dimensional Analyses of Human Organogenesis. , 2022, , 107-112.		0
5	Nascent nephrons during human embryonic development: Spatial distribution and relationship with urinary collecting system. Journal of Anatomy, 2021, 238, 455-466.	1.5	1
6	Bronchial tree of the human embryo: Categorization of the branching mode as monopodial and dipodial. PLoS ONE, 2021, 16, e0245558.	2.5	6
7	Morphology and morphometry of the human early foetal brain: A threeâ€dimensional analysis. Journal of Anatomy, 2021, 239, 498-516.	1.5	8
8	Early development of the cortical layers in the human brain. Journal of Anatomy, 2021, 239, 1039-1049.	1.5	6
9	Upper arm posture during human embryonic and fetal development. Anatomical Record, 2021, , .	1.4	2
10	Position of the cecum in the extraembryonic and abdominal coelom in the early fetal period. Congenital Anomalies (discontinued), 2020, 60, 87-88.	0.6	0
11	Vesicular swelling in the cervical region with lymph sac formation in human embryos. Congenital Anomalies (discontinued), 2020, 60, 62-67.	0.6	2
12	Running course of the colon during the embryonic period. Clinical Anatomy, 2020, 33, 628-629.	2.7	0
13	Relationship between rectal abdominis muscle position and physiological umbilical herniation and return: A morphological and morphometric study. Anatomical Record, 2020, 303, 3044-3051.	1.4	3
14	Development of Helical Myofiber Tracts in the Human Fetal Heart: Analysis of Myocardial Fiber Formation in the Left Ventricle From the Late Human Embryonic Period Using Diffusion Tensor Magnetic Resonance Imaging. Journal of the American Heart Association, 2020, 9, e016422.	3.7	12
15	Shoulder girdle formation and positioning during embryonic and early fetal human development. PLoS ONE, 2020, 15, e0238225.	2.5	6
16	Threeâ€dimensional morphogenesis of the omental bursa from four recesses in staged human embryos. Journal of Anatomy, 2020, 237, 166-175.	1.5	6
17	The bronchial tree of the human embryo: an analysis of variations in the bronchial segments. Journal of Anatomy, 2020, 237, 311-322.	1.5	12
18	Shoulder girdle formation and positioning during embryonic and early fetal human development. , 2020, 15, e0238225.		0

Τετςυγά Τακακύψα

#	Article	IF	CITATIONS
19	Shoulder girdle formation and positioning during embryonic and early fetal human development. , 2020, 15, e0238225.		0
20	Shoulder girdle formation and positioning during embryonic and early fetal human development. , 2020, 15, e0238225.		0
21	Shoulder girdle formation and positioning during embryonic and early fetal human development. , 2020, 15, e0238225.		Ο
22	Relationship Between Physiological Umbilical Herniation and Liver Morphogenesis During the Human Embryonic Period: A Morphological and Morphometric Study. Anatomical Record, 2019, 302, 1968-1976.	1.4	5
23	Rib Cage Morphogenesis in the Human Embryo: A Detailed Threeâ€Đimensional Analysis. Anatomical Record, 2019, 302, 2211-2223.	1.4	13
24	Human embryonic ribs all progress through common morphological forms irrespective of their position on the axis. Developmental Dynamics, 2019, 248, 1257-1263.	1.8	3
25	Morphogenesis of the femur at different stages of normal human development. PLoS ONE, 2019, 14, e0221569.	2.5	15
26	Return of the intestinal loop to the abdominal coelom after physiological umbilical herniation in the early fetal period. Journal of Anatomy, 2019, 234, 456-464.	1.5	12
27	Level set distribution model of nested structures using logarithmic transformation. Medical Image Analysis, 2019, 56, 1-10.	11.6	3
28	Spatial Relationship Between the Metanephros and Adjacent Organs According to the Carnegie Stage of Development. Anatomical Record, 2019, 302, 1901-1915.	1.4	3
29	Revisiting the infracardiac bursa using multimodal methods: topographic anatomy for surgery of the esophagogastric junction. Journal of Anatomy, 2019, 235, 88-95.	1.5	7
30	Critical Growth Processes for the Midfacial Morphogenesis in the Early Prenatal Period. Cleft Palate-Craniofacial Journal, 2019, 56, 1026-1037.	0.9	12
31	Spatiotemporal Statistical Model of Anatomical Landmarks on a Human Embryonic Brain. Lecture Notes in Computer Science, 2019, , 94-103.	1.3	0
32	Variations of the Circle of Willis at the End of the Human Embryonic Period. Anatomical Record, 2018, 301, 1312-1319.	1.4	10
33	3D Analysis of Human Embryos and Fetuses Using Digitized Datasets From the Kyoto Collection. Anatomical Record, 2018, 301, 960-969.	1.4	9
34	Morphogenesis of the Middle Ear during Fetal Development as Observed Via Magnetic Resonance Imaging. Anatomical Record, 2018, 301, 757-764.	1.4	4
35	Tail reduction process during human embryonic development. Journal of Anatomy, 2018, 232, 806-811.	1.5	9
36	Formation of the Periotic Space During the Early Fetal Period in Humans. Anatomical Record, 2018, 301, 563-570.	1.4	8

Τετςυγά Τακακύψα

#	Article	IF	CITATIONS
37	Blechschmidt Collection: Revisiting specimens from a historical collection of serially sectioned human embryos and fetuses using modern imaging techniques. Congenital Anomalies (discontinued), 2018, 58, 152-157.	0.6	14
38	A Spatiotemporal Statistical Shape Model of the Brain Surface during Human Embryonic Development. Advanced Biomedical Engineering, 2018, 7, 146-155.	0.6	6
39	Branching morphogenesis of the urinary collecting system in the human embryonic metanephros. PLoS ONE, 2018, 13, e0203623.	2.5	8
40	Positional Changes of the Ocular Organs During Craniofacial Development. Anatomical Record, 2017, 300, 2107-2114.	1.4	7
41	Dynamics of gyrification in the human cerebral cortex during development. Congenital Anomalies (discontinued), 2017, 57, 8-14.	0.6	4
42	A Spatiotemporal Statistical Model for Eyeballs of Human Embryos. IEICE Transactions on Information and Systems, 2017, E100.D, 1505-1515.	0.7	7
43	Cartilage formation in the pelvic skeleton during the embryonic and early-fetal period. PLoS ONE, 2017, 12, e0173852.	2.5	9
44	Statistical Shape Model of Nested Structures Based on the Level Set. Lecture Notes in Computer Science, 2017, , 169-176.	1.3	2
45	Correlation of external ear auricle formation with staging of human embryos. Congenital Anomalies (discontinued), 2016, 56, 86-90.	0.6	5
46	Formation of the circle of Willis during human embryonic development. Congenital Anomalies (discontinued), 2016, 56, 233-236.	0.6	11
47	MR Imaging of the Pituitary Gland and Postsphenoid Ossification in Fetal Specimens. American Journal of Neuroradiology, 2016, 37, 1523-1527.	2.4	4
48	Intestinal Rotation and Physiological Umbilical Herniation During the Embryonic Period. Anatomical Record, 2016, 299, 197-206.	1.4	28
49	The Digestive Tract and Derived Primordia Differentiate by Following a Precise Timeline in Human Embryos Between Carnegie Stages 11 and 13. Anatomical Record, 2016, 299, 439-449.	1.4	8
50	The Germ Cell Fate of Cynomolgus Monkeys Is Specified in the Nascent Amnion. Developmental Cell, 2016, 39, 169-185.	7.0	252
51	A Novel Strategy to Reveal the Latent Abnormalities in Human Embryonic Stages from a Large Embryo Collection. Anatomical Record, 2016, 299, 8-24.	1.4	11
52	Morphogenesis of the middle ear ossicles and spatial relationships with the external and inner ears during the embryonic period. Anatomical Record, 2016, 299, 1325-1337.	1.4	10
53	Morphometric human embryonic brain features according to developmental stage. Prenatal Diagnosis, 2016, 36, 338-345.	2.3	3
54	3D models related to the publication: Morphogenesis of the liver during the human embryonic period. MorphoMuseuM, 2016, 1, e1.	0.2	1

Τετςυγά Τακακύψα

#	Article	IF	CITATIONS
55	3D models related to the publication: Morphogenesis of the stomach during the human embryonic period. MorphoMuseuM, 2016, 1, e3.	0.2	1
56	Morphological features and length measurements of fetal lateral ventricles at 16–25 weeks of gestation by magnetic resonance imaging. Congenital Anomalies (discontinued), 2015, 55, 99-102.	0.6	7
57	Morphogenesis of the Inner Ear at Different Stages of Normal Human Development. Anatomical Record, 2015, 298, 2081-2090.	1.4	30
58	Three-dimensional morphology of the human embryonic brain. Data in Brief, 2015, 4, 116-118.	1.0	4
59	Morphology and morphometry of the human embryonic brain: A three-dimensional analysis. NeuroImage, 2015, 115, 96-103.	4.2	30
60	Morphogenesis of the Spleen During the Human Embryonic Period. Anatomical Record, 2015, 298, 820-826.	1.4	16
61	Spatial Change of Cruciate Ligaments in Rat Embryo Knee Joint by Three-Dimensional Reconstruction. PLoS ONE, 2015, 10, e0131092.	2.5	4
62	3D models related to the publication: Morphology of the human embryonic brain and ventricles. MorphoMuseuM, 2015, 1, e3.	0.2	1
63	3D models related to the publication: Morphogenesis of the inner ear at different stages of normal human development. MorphoMuseuM, 2015, 1, e6.	0.2	0
64	Three-dimensional reconstruction of rat knee joint using episcopic fluorescence image capture. Osteoarthritis and Cartilage, 2014, 22, 1401-1409.	1.3	8
65	Morphology and morphometry of fetal liver at 16–26 weeks of gestation by magnetic resonance imaging: Comparison with embryonic liver at <scp>C</scp> arnegie stage 23. Hepatology Research, 2013, 43, 639-647.	3.4	6
66	Morphogenesis of Lateral Choroid Plexus During Human Embryonic Period. Anatomical Record, 2013, 296, 692-700.	1.4	13
67	Threeâ€dimensional models once again: For research and teaching of early human development. Congenital Anomalies (discontinued), 2013, 53, 58-59.	0.6	2
68	Morphometric analysis of the brain vesicles during the human embryonic period by magnetic resonance microscopic imaging. Congenital Anomalies (discontinued), 2012, 52, 55-58.	0.6	18
69	Movement of the external ear in human embryo. Head & Face Medicine, 2012, 8, 2.	2.1	24
70	Embryonic Liver Morphology and Morphometry by Magnetic Resonance Microscopic Imaging. Anatomical Record, 2012, 295, 51-59.	1.4	18
71	Aberrant somatic hypermutations in thyroid lymphomas. Leukemia Research, 2009, 33, 649-654.	0.8	14
72	Polymerase chain reaction-based clonality analysis in thyroid lymphoma. International Journal of Molecular Medicine, 2002, 10, 113-7.	4.0	8

#	Article	IF	CITATIONS
73	DNA Sequence of Immunoglobulin Heavy Chain Variable Region Gene in Thyroid Lymphoma. Japanese Journal of Cancer Research, 2001, 92, 1041-1047.	1.7	5
74	The return process of physiological umbilical herniation in human fetuses: The possible role of the vascular tree and umbilical ring. Journal of Anatomy, 0, , .	1.5	0